Journal of Petroleum Science and Technology 12(3): 35, 2022, Pages 12-17
DOI:10.22078/JPST.2023.4879.1821

Journal of Petroleum Science and Technology

Research Paper

https://jpst.ripi.ir/

Development of an Artificial Neural Network Model to Calculate Static Young's Modulus Based on a Log-derived Data Base

Samir Khaled[1, 2], Sayed Gomaa[1, 2], Karim Nasr[1]*, Mohamed Elwageeh[2, 3] and Salah Bader[1]

1. Mining and Petroleum Engineering Department, Faculty of Engineering, Al-Azhar University, Cairo, Egypt

2. Petroleum Engineering and Gas Technology Department, Faculty of Energy and Environmental Engineering, British University in Egypt (BUE), El Sherouk City, Cairo, Egypt

3. Mining, Petroleum and Metallurgy Engineering Department, Cairo University, Cairo, Egypt

Abstract

Static Young's Modulus is a measure of reservoir rock stiffness and is best determined by experimental studies on cores. However, the experimental procedures are demanding with considerable cost. On the other hand, a dynamic Young's modulus can easily be estimated from readily available petrophysical data. The static young's modulus can easily be obtained from the dynamic counterpart by empirical relationships. This research attempts to use AI techniques to predict Static Young's modulus. Two thousand three hundred fifty data sets were collected from several wells in the Middle East with sandstone and limestone lithology and used to build an AI model. Each data set contains static Young's Modulus as a function of the bulk density, shear wave arrival time, and compressional wave arrival time. An artificial neural network (ANN) model was developed to predict the static young's modulus with high accuracy of $R^2 = 0.999$ and AARE of 0.028%. The proposed model was validated with measured reservoir rock data and was compared with four different correlations. The results showed that the model provided the highest coefficient of determination (R^2) and the lowest standard deviation.

Keywords: Young's Modulus, Neural Network, Bulk Density, Shear Wave Arrival Time, Compressional Wave Arrival Time.

Introduction

Young's modulus and Poisson's ratio are two rock properties often used to estimate in situ stresses and wellbore stability analysis, [1,2] reservoir compaction survey, and prediction of optimum drilling mud pressure. When drilling hydrocarbon wells, the static Young's modulus (E_{static}) parameter is used to describe the *in situ* stresses of the well in addition to the mechanical and petro-physical properties, and the results ensure wellbore stability [3]. However, static measurement tests are notoriously difficult since they necessitate adequate rock core quality, which isn't always available. Instead, the dynamic elastic parameters, which are highly influenced by the pores and cracks, can be discovered using ultrasonic testing on well log data, which is always available in the oil industry [4].

The dynamic Young's modulus ($E_{dynamic}$) is 1.5 to 3 times less than the Estatic. The huge disparity between the two testing procedures is related to a difference in strain amplitude, according to tests. Small strain amplitude oscillations are used to acquire the dynamic moduli, while relatively large amplitudes and slowly increasing stresses are used to obtain the static moduli. Additionally, there is a considerable change in parameter values obtained during the first loading and values observed during successive loading cycles for the static moduli [5].

Static measurements take a long time and are not cost-effective. Due to these challenges, theoretical models and correlations for determining rock's mechanical properties directly from well logs have been created [6]. The difference between the E_{static} and $E_{dynamic}$ derives from the energy loss caused by the reflection and refraction at the rock interface as the wave pulse moves through the rock pores [7].

The static elastic modulus of Microcline Granite can be derived using the dynamic elastic modulus (as seen in Equation 1) [8].

$$E_{static} = (1.137\, E_{dynamic}) - 9.685 \tag{1}$$

For clay rock and wet soil, two empirical correlations were established to estimate Estatic using Equations 2 and 3 [9].

$$E_{static} = (0.033\, E_{dynamic}) + 0.0065 \tag{2}$$

**Corresponding author:* Karim Nasr, Mining and Petroleum Engineering Department, Faculty of Engineering, Al-Azhar University, Cairo, Egypt

E-mail addresses: Karim.nasr@bue.edu.eg

Received 2022-08-14, Received in revised form 2023-01-24, Accepted 2023-02-12, Available online 2023-05-24

$E_{static} = (0.061\ E_{dynamic}) + 0.00285$ (3)

King developed a correlation for calculating E_{static} in igneous and metamorphic rocks (as seen in Equation 4). He also stated that the difference between modulus is readily visible in soft rocks (sandstone) against hard rocks (granite) in the Canadian shield rocks [10].

$E_{static} = (1.263\ E_{dynamic}) -29.5$ (4)

The dynamic elastic modulus ($E_{dynamic}$) and formation density can also be used to compute Estatic (as seen in Equation 5) [11].

$\log(E_{static}) = 0.02 + 0.77\log(\gamma E_{dynamic})$ (5)

E_{static} can be predicted from $E_{dynamic}$ using geotechnical and geophysical data gathered from boreholes excavated by the British geological survey, most of which are Jurassic in age. The geophysical logs were used to determine $E_{dynamic}$ in the borehole. It necessitates using the sonic log to calculate V_p and shear V_s wave velocity as well as the gamma log to determine formation density using Equation 6 [12].

$E_{static} = (0.69\ E_{dynamic}) + 6.4$ (6)

E_{static} is connected to porosity. The gap between the E_{static} and $E_{dynamic}$ grows with porosity increase and becomes more substantial for greater porosities, according to a series of studies performed on high permeability cores [13].

$E_{static} = (0.956\ E_{dynamic}) -0.69$ (7)

or soft and hard rocks, Wang estimated Estatic from $E_{dynamic}$. They concluded that Young's modulus for soft formations ranges from 1000,000 to 1,000,000 psi. For medium formation, the modulus is 2,000,000 to 10,000,000 psi, while the modulus reaches 12,000,000 psi for hard formation [14].

$E_{static} = E_{dynamic} -15.2$ (8)

Fei et al. established an empirical correlation based on tests done on core samples from tight sandstone reservoirs to predict E_{static} from $E_{dynamic}$ [15].

$E_{static} = (0.546\ E_{dynamic}) -3.4941$ (9)

Najibi et al. derived two empirical equations to predict Estatic. If, V_s is unavailable, the first empirical equation was developed using limestone core specimens. The second developed correlation employs the compressional velocity (V_p) to forecast the E_{static} values [16].

$E_{static} = 0.014{*}E_{dynamic}^{1.96}$ (10)

$E_{static} = 0.169{*}V_p^{3.24}$ (11)

Elkatany et al. developed an equation that relies on wireline information and doesn't require the knowledge of $E_{dynamic}$. The bulk density(ρ_b), were used as independent variables, whereas compressional (V_p) and shear (V_s) transit times, as well as Young's modulus, was used as dependent variable. They also claimed that data clustering enhances E_{static} prediction accuracy [17]. Estatic values vary significantly between formations, necessitating the estimation of E_{static} along multiple parts of the drilled well [18].

$lnE_{static} = 14.9\text{-}0.61ln(V_p)\text{-}2.18ln(V_s) + 1.42ln\rho_b$ (12)

$lnEstatic = 14.845619\text{-}0.613326ln(V_p)\ \text{-}2.179364ln(V_s) +1.417512ln\rho_b$ (13)

Abdulraheem et al. improved three machine learning models without specifying rock formation type to calculate E_{static} and the static Poison's ratio. In addition, the ability of the generated models to estimate reservoir rock mechanical properties was proven [19].

Tariq et al. developed an accurate model for E_{static} prediction using wireline logs input. Their conclusion stated that an artificial neural network best fits their suggested model is artificial neural network [20].

Rashidi et al. investigated the precision of ANN-based correlation between E_{static} and $E_{dynamic}$ for limestone formation. The findings revealed that ANN is an effective tool for predicting data in situations where some parameter data have no relationship. It can also generate specialized lithological correlations to evaluate static elastic modulus data derived from dynamic Young's modulus data [21].

From conventional well logs, Mahmoud et al. employed artificial neural networks (ANN) to estimate E_{static} for sandstone formation. Values of compressional (V_p) and shear (V_s) transit times, as well as bulk density(ρb) were used to predict E_{static} [22].

Elkatany et al. built an artificial intelligence model to predict the E_{static} using measured core data. Their results showed that artificial neural network (ANN) is the best artificial intelligence technique compared to other methods [23].

Badrouchi et al. used core samples from eight different drilled wells to estimate the elastic properties of the Bakken formation using an artificial neural network (ANN). The neural network was trained using bulk density (ρ_b) and compressional (V_p) and shear (V_s) wave velocities. Their results demonstrated that ANN could better predict E_{static} than the correlation method [24].

E_{static} Prediction Methodology

The preparation and processing of data is a critical phase in building any ANN-based mathematical model. The quality and number of data points used in the developed model determine its performance. As acquiring elastic parameters using triaxial tests on cores in the laboratory is quite expensive, well log data are used as input for the developed model. The wireline log data used are gamma ray, neutron porosity, bulk density, shear, and compressional wave arrival time.

Data Description and Analysis

In this study, 2350 data sets of Young's modulus as a function of the gamma-ray, neutron porosity, bulk density (ρ_b), in g/cm^3, shear wave arrival time (V_s), µs/ft and compressional wave arrival time (V_p), µs/ft, are collected from various Middle E_{astern} wells with limestone and sandstone lithology. The bulk density was found to have a standard deviation of 0.06 and a sample variance of 0. The neutron porosity's standard deviation and sample variance were 0.08 and 0.01, respectively. The standard deviation for shear and compressional wave velocity was 0.22 and 0.36, respectively. At the same time, the sample variance for shear wave velocity and compressional wave velocity were 0.05 and 0.13, respectively. The Estatic had a standard deviation of 1.95 and a sample variance of 3.80. Table 1 presents a detailed statistical description of the data.

70% (1644 datasets) of the data were set as a training data, 15% (353 datasets) were set as a validation data to develop the model and the last 15% (353 datasets) was used for testing the model performance which is presented in this manuscript. The objective is to find the best artificial intelligence model for predicting accurate E_{static}, defined as having the highest R and the lowest AAPE. In addition, the artificial neural network technique (ANN) was used to develop new empirical correlation based on the best combinations of the available logs.

Table 1 Statistical description of 2350 data points.

Parameter	Mean	Median	Mode	Minimum	Maximum	Range	Standard Deviations	Sample Variance	Skewness	Kurtosis
RHOB (g/cm^3)	2.53	2.53	2.54	2.39	2.85	0.47	0.06	0.00	0.12	1.35
Porosity	0.30	0.296	0.30	0.06	0.46	0.40	0.08	0.01	-0.50	0.07
GR	86.53	73.85	71.26	12.09	176.75	164.67	34.99	1,224	0.79	-0.38
V_s (µs/ft)	1.81	1.75	1.74	1.38	2.93	1.55	0.22	0.05	1.41	3.20
V_p (µs/ft)	3.46	3.44	3.43	2.70	5.39	2.69	0.36	0.13	1.073	-3.20
E_{static} (GPa)	6.08	5.53	5.23	3.10	20.87	17.77	1.95	3.80	2.44	9.57

Building Model Using AI Techniques

In Figure 1, it is indicated that Young's modulus correlates with the bulk density (ρ_b), neutron porosity, gamma ray, shear wave arrival time (V_s) and Compressional wave arrival time (V_P), with correlation coefficients of 0.67, -0.78, -0.60, 0.98, and 0.94, respectively. As a result, the parameters which have the highest correlation coefficient with E_{static}, are chosen to simplify the model. These are the bulk density, compressional wave, and shear wave velocity.

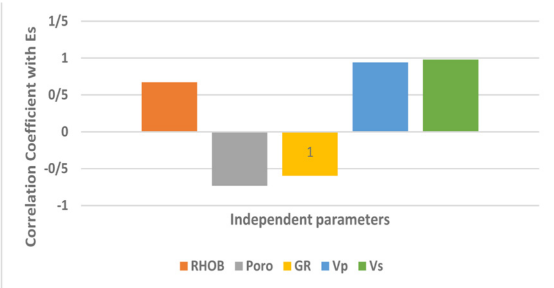

Fig. 1 Correlating Young's modulus with input parameters.

The model consists of an input layer; the first layer consists of three neurons. The second layer, which is the hidden layer, includes ten neurons. Last, the output layer, the third layer, consist of only one neuron for the output parameter.

Mathematical Model Development Using ANN

After several trials, it was discovered that for the training algorithm, a Levenberg-Marquadt technique is the best, the sigmoid function is used as a transfer function for the hidden layer, and the pure linear is used for the output function. The developed neural network model is described in Table 2.

Table 2 Neural network model complete description.

Neural Network Parameters	Description
Number of inputs	3
Number of outputs	1
Number of neurons in the hidden layer	10
Number of the hidden layer (s)	1
Training algorithm	Levenberg-Marquardt
Hidden layer transfer function	Logistic Sigmoid
Outer layer transfer function	Pure linear
Training percentage	70
Testing percentage	15
Validation percentage	15

The weights and biases between the input, hidden layers, and outputs are shown in Table 3. The inputs for the hidden layer using ANN as the developed model are calculated using Equation 14 and expressed as;

$$S_{i,j} = \sum_{j=1}^{N} (w_{ij}, x_j) + b_i \quad (14)$$

Table 3 Weights between the input, hidden layers, and outputs.

Neuron #	$w_{i,j=1}$	$w_{i,j=2}$	$w_{i,j=3}$	b_i	w_{hoi}	b_{ho}
1	1.3952	-2.5985	3.8647	-6.0262	-0.5619	-0.44077
2	-0.00875	2.7266	-2.7206	-4.4192	-3.047	
3	-3.4199	1.8286	2.3013	2.5262	0.010348	
4	3.3734	0.79317	2.7589	-2.8637	-0.00573	
5	0.2248	0.90683	0.32589	-2.5864	6.4313	
6	-0.12404	-1.4146	0.48188	-0.12676	-1.1801	
7	-0.27375	0.12288	1.7617	0.12739	0.19753	
8	0.8954	4.8995	-1.6576	1.8017	-0.00573	
9	3.641	1.8059	0.84416	5.8678	-0.00468	
10	1.0974	3.8853	-3.3913	7.015	0.1677	

Where x_j represents the normalized ρ_b, Vp and V_s, respectively. The normalized ρ_b, V_p and V_s can be calculated using Equations 15, 16, and 17 respectively;

$$\rho_b n = 4.301075\rho_b - 11.25806 \quad (15)$$

$$V_P^n = 0.743771 V_P - 3.009669 \quad (16)$$

$$V_S^n = 1.29199 V_S - 2.784238 \quad (17)$$

The static Young's modulus can be calculated by the following functions using Equation 18;

$$E_{Static} = 8.887\left[\sum_{i=1}^{n} \left(\frac{W_{hoi}}{1+ex(-S_i)}\right) + b_{ho}\right] + 11.986 \quad (18)$$

Results and Discussion

Validation and comparison

Figure 2 shows the cross plots of the efficiency of the network. For an ideal fit, the data points should fall around the line of the unit slope, where the network results are equal to the targets. For more validation of the proposed model, we used 45 unseen data sets taken from Najibi et al. As a result, the proposed model predicted the value of Estatic with a high coefficient of determination (R^2) as shown in Figure 3.

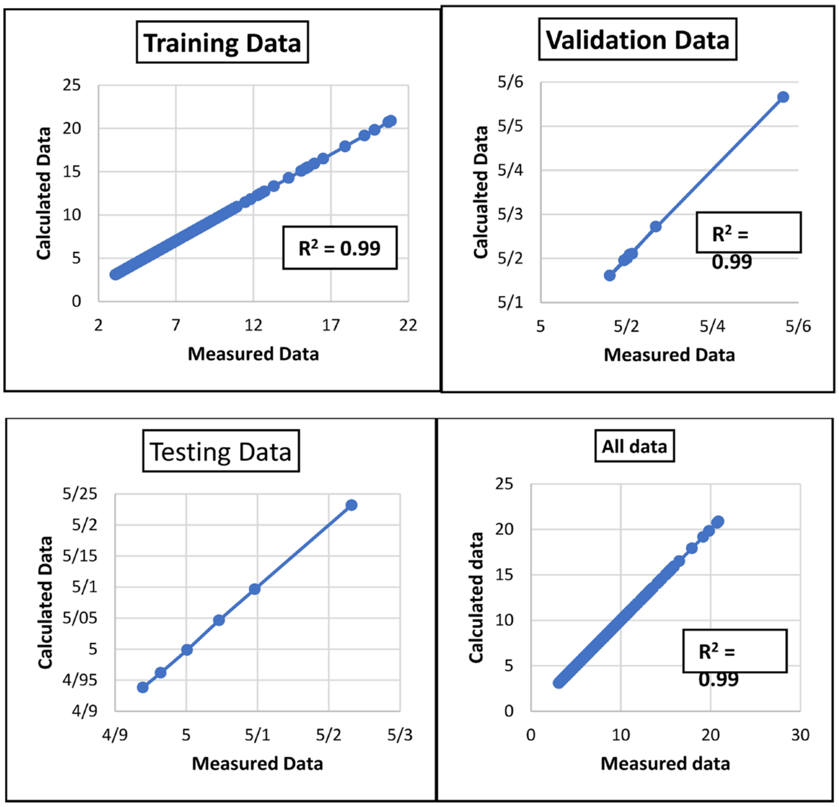

Fig. 2 Cross plots of the efficiency of the network.

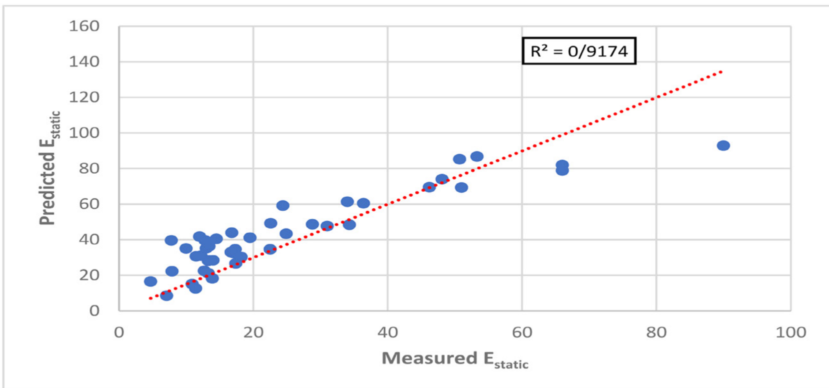

Fig. 3 Model Validation using Najibi measured data.

Table 4 and Figures 4 - 7 conclude the results of 4 correlations analysis which have been used to conduct the comparison with the developed correlation. The proposed correlation has the highest coefficient of determination (R^2) and lowest standard deviation according to the results. In addition, compared to the other correlations, the proposed model has the lowest ARE and AARE.

Table 4 Comparison between the proposed model and other correlations.

Correlation #	Author (s)	R^2	SD	RMSE	ARE	AARE
1	[?] Eissa and Kazi (1988)	0.876	9.247	2.122	76.366	76.366
2	[?] Belikov et al. (1962)	0.877	6.71	10.333	144.410	144.410
3	[?] Najibi et al. (2015)	0.883	3.53	5.208	14.684	14.684
4	[?] Fei et al. (2016)	0.972	2.89	5.158	37.873	37.873
5	Our Correlation	0.999	0.028	2.83E-06	0.0281	0.0281

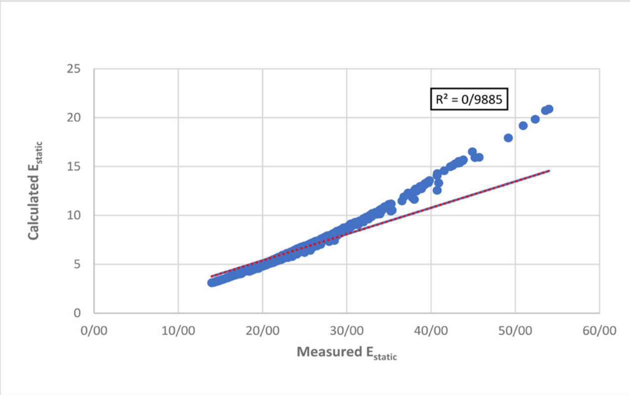

Fig. 4 Testing published correlation 1.

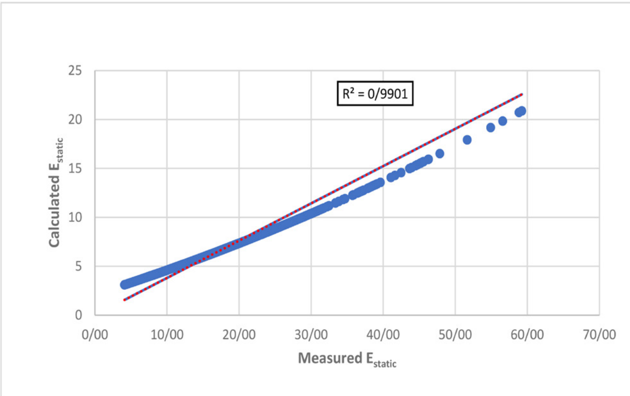

Fig. 5 Testing published correlation 2.

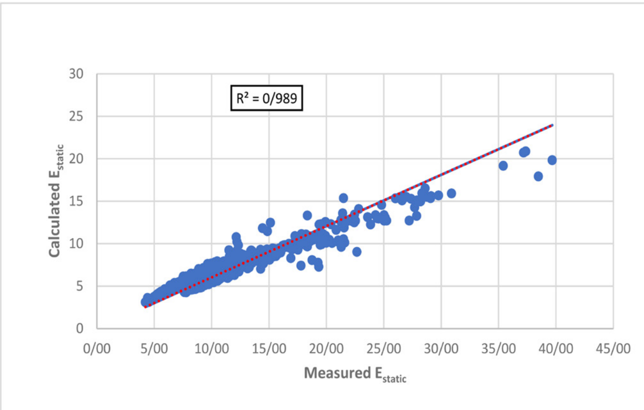

Fig. 6 Testing published correlation 3.

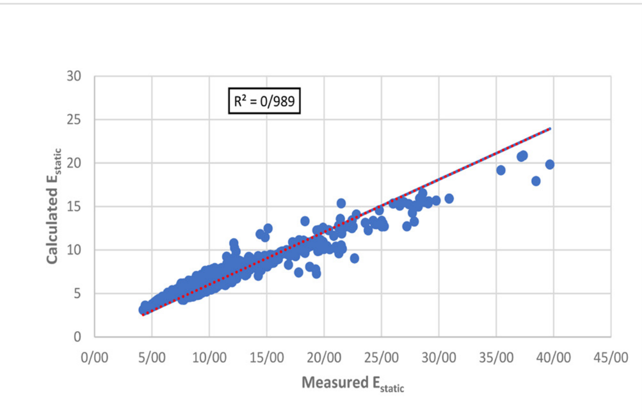

Fig. 7 Testing published correlation 4.

Conclusions

An artificial neural network model was developed to calculate the Estatic based on 2350 data sets of Young's modulus as a function of bulk density, VP, and Vs that were collected from different wells in the Middle East. This model was compared with other published empirical correlations and AI-based models. The proposed ANN-based model calculates Young's modulus with high accuracy, achieving a coefficient of determination of 0.999 with an absolute average relative error of 0.028 %.

Acknowledgments

The authors thank anonymous reviewers for their valuable comments.

Nomenclatures

bi, bias between input and hidden layers of neural network for ifh neuron; bho, bias between hidden and output layers of neural network;
J, total number of input parameters;
N, total number of neurons;
R, correlation coefficient;
R2, coefficient of determination;
wi j, weights vector between input and hidden layers of neural network;
whoi, Weights vector between hidden and output layers of neural network.

References

1. Abdulraheem A, Ahmed M, Vantala A, Parvez T (2009) Prediction of rock mechanical parameters for hydrocarbon reservoirs using different artificial intelligence techniques, In SPE Saudi Arabia Section Technical Symposium, OnePetro, doi.org/10.2118/126094-MS.
2. Alramahi B A, Alshibli K A, Attia A M (2005) Influence of grain size and consolidation pressure on porosity of rocks, In Site Characterization and Modeling, 1-13, doi.org/10.1061/40785(164)41.
3. Alshibli K A, Alramahi B A, Attia A M (2006) Assessment of spatial distribution of porosity in synthetic quartz cores using microfocus computed tomography (μCT), Particulate science and technology, 24, 4: 369-380, doi.org/10.1080/02726350600934606.
4. Nes O M, Fjær E, Tronvoll J, Kristiansen T G, Horsrud P (2012) Drilling time reduction through an integrated rock mechanics analysis, Journal of Energy Resources Technology, 134: 3, doi.org/10.1115/1.4006866.
5. Fjar E, Holt R M, Raaen A, Horsrud P (2008) Petroleum related rock mechanics, Elsevier.
6. Lacy L L (1997) Dynamic rock mechanics testing for optimized fracture designs, In SPE Annual Technical Conference and Exhibition, OnePetro, doi.org/10.2118/38716-MS.
7. Brandas L T, Fjaer E, Tokle K, Tronvoll J (2012) Relating acoustic wave velocities to formation mechanical properties, In 46th US Rock Mechanics/Geomechanics Symposium, OnePetro.
8. Zisman, W. (1933) Comparison of the statically and seismologically determined elastic constants of rocks,

Proceedings of the National Academy of Sciences of the United States of America, 19, 7: 680, doi.org/10.1073/pnas.19.7.680.

9. Belikov B (1962). Elastic properties of rocks, Studia Geophysica et Geodaetica 6, 1: 75-85.
10. Goryainov N N, Lyakhovitskii F M (1979) Seismic methods in engineering geology, Seismicheskie metody v inzhenernoi geologii.
11. King M S (1983) Static and dynamic elastic properties of igneous and metamorphic rocks from the Canadian shield.
12. Eissa E, Kazi A (1988) Relation between static and dynamic Young's moduli of rocks, International Journal of Rock Mechanics and Mining and Geomechanics Abstracts, 25: 6.
13. McCann D, Entwisle D (1992) Determination of Young's modulus of the rock mass from geophysical well logs, Geological Society, London, Special Publications, 65, 1: 317-325, doi.org/10.1144/GSL.SP.1992.065.01.2.
14. Morales R H, Marcinew R P (1993) Fracturing of high-permeability formations: mechanical properties correlations, In SPE Annual Technical Conference and Exhibition, OnePetro, doi.org/10.2118/26561-MS.
15. Wang Z (2000) Dynamic versus static elastic properties of reservoir rocks, Seismic and acoustic velocities in reservoir rocks, 3: 531-539.
16. Fei W, Huiyuan B, Jun Y, Yonghao Z (2016) Correlation of dynamic and static elastic parameters of rock, Electronic Journal of Geotechnical Engineering, 21, 04: 1551-1560.
17. Najibi A R, Ghafoori M, Lashkaripour G R, Asef M R (2015) Empirical relations between strength and static and dynamic elastic properties of Asmari and Sarvak limestones, two main oil reservoirs in Iran, Journal of Petroleum Science and Engineering, 126: 78-82, doi.org/10.1016/j.petrol.2014.12.010.
18. Elkatatny S, Mahmoud M, Mohamed I, Abdulraheem A (2018) Development of a new correlation to determine the static Young's modulus, Journal of Petroleum Exploration and Production Technology, 8, 1: 17-30, doi.org/10.1007/s13202-017-0316-4.
19. Mahmoud A A, Elkatatny S, Al-Shehri D (2020) Application of machine learning in evaluation of the static young's modulus for sandstone formation, Sustainability, 12, 5: 1880, doi.org/10.3390/su12051880.
20. Elkatatny S, Tariq Z, Mahmoud M, Abdulraheem A, Mohamed I (2019) An integrated approach for estimating static Young's modulus using artificial intelligence tools, Neural Computing and Applications, 31, 8: 4123-4135, doi.org/10.1007/s00521-018-3344-1.
21. Tariq Z, Elkatatny S, Mahmoud M, Abdulraheem A (2016) A holistic approach to develop new rigorous empirical correlation for static Young's modulus, In Abu Dhabi International Petroleum Exhibition and Conference, OnePetro, doi.org/10.2118/183545-MS.
22. Rashidi M, Hajipour M, Asadi A (2018) Correlation between static and dynamic elastic modulus of limestone formations using artificial neural networks, In 52nd US Rock Mechanics/Geomechanics Symposium, OnePetro.
23. Mahmoud A A, Elkatatny S, Ali A, Moussa T (2019) Estimation of static young's modulus for sandstone formation using artificial neural networks, Energies, 12, 11: 2125, doi.org/10.3390/en12112125.
24. Badrouchi F, Badrouchi N, Rabiei M, Rasouli V (2019) Estimation of elastic properties of bakken formation using an artificial neural network model, In 53rd US Rock Mechanics/Geomechanics Symposium, OnePetro.